

UC Irvine

UC Irvine Previously Published Works

Title

Unexpected hydroxyl radical production in brewed tea under sunlight.

Permalink

<https://escholarship.org/uc/item/0ts1k4w9>

Journal

PNAS Nexus, 3(1)

Authors

Qin, Linjun

Yang, Lili

Shiraiwa, Manabu

et al.

Publication Date







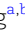
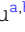


2024

DOI

10.1093/pnasnexus/pgae015

Peer reviewed

Unexpected hydroxyl radical production in brewed tea under sunlight

Linjun Qin ^{a,b}, Lili Yang ^{a,b,*}, Manabu Shiraiwa ^c, Francesco Faiola ^{a,b}, Huan Zhong ^d, Christian Sonne ^e, Yujue Yang ^{a,b}, Shuting Liu ^{a,b}, Guorui Liu ^{a,b,f,*}, Minghui Zheng ^{a,b,f} and Guibin Jiang ^{a,b,f}

^aState Key Laboratory of Environmental Chemistry and Ecotoxicology, Research Center for Eco-Environmental Sciences, Chinese Academy of Sciences, Beijing 100085, China

^bCollege of Resources and Environment, University of the Chinese Academy of Sciences, Beijing 100190, China

^cDepartment of Chemistry, University of California, Irvine, CA 92697, USA

^dState Key Laboratory of Pollution Control and Resources Reuse, School of the Environment, Nanjing University, Nanjing 210023, China

^eDepartment for Bioscience, Arctic Research Centre, Aarhus University, Roskilde DK-4000, Denmark

^fInstitute of Environment and Health, Hangzhou Institute for Advanced Study, University of the Chinese Academy of Sciences, Hangzhou 310024, China

*To whom correspondence should be addressed: Email: lyang@rcees.ac.cn (L.Y.); Email: grliu@rcees.ac.cn (G.L.)

Edited By: Yi-Jun Xu

Abstract

Tea is one of the world's most popular and widely consumed beverages. It is a common pastime to enjoy a cup of tea in the sunshine. However, little attention has been given to understanding the possible photochemical reactions occurring beneath the calm surface of brewed tea. Epigallocatechin gallate (EGCG), which is widely used in food and beverages, is the most significant active ingredient found in tea. In this study, we investigated the presence of free radicals in both an aqueous EGCG solution and brewed tea under simulated sunlight conditions. To our surprise, we unexpectedly observed the production of hydroxyl radicals ($\bullet\text{OH}$) in brewed tea. It was found that sunlight irradiation played a critical role in the formation of $\bullet\text{OH}$, independent of the presence of metal ions. Furthermore, we demonstrated that the $\bullet\text{OH}$ generated from the EGCG aqueous solution induced cell cytotoxicity and DNA damage in vitro. Considering the crucial role of $\bullet\text{OH}$ in various fields, including human health and the environment, it is important to further explore the practical implications of $\bullet\text{OH}$ production in brewed tea under sunlight. In summary, our study unveils the unexpected formation of $\bullet\text{OH}$ in brewed tea and emphasizes the significance of sunlight-induced reactions. The observed cytotoxic and DNA-damaging effects of $\bullet\text{OH}$ emphasize the importance of understanding the potential health consequences associated with tea consumption. Further research in this area will contribute to a better understanding of the broader implications of $\bullet\text{OH}$ production in brewed tea under sunlight.

Significance Statement

Enjoying a cup of tea in the sunshine is a popular activity. Although tea consumption is considered beneficial for human health because of the important bioactive ingredients, especially epigallocatechin gallate (EGCG), some studies have suggested that tea could have conflicting effects. Free radical chemistry is the core of understanding the health effects of EGCG in tea. Here, in addition to hydrogen radicals ($\bullet\text{H}$), hydroxyl radicals ($\bullet\text{OH}$) were unexpectedly produced in aqueous EGCG solution and brewed tea under sunlight irradiation. The $\bullet\text{OH}$ is considered the most damaging reactive species. We reveal that the $\bullet\text{OH}$ production in brewed tea and EGCG under sunlight could have potential health effects. Therefore, people must recognize the tea drinking under sunlight.

Introduction

Tea is one of the most widely consumed beverages, and the tea plant (*Camellia sinensis*) is cultivated in >30 countries worldwide (1). Tea drinking is considered beneficial for human health because it can improve mental health and potentially prevent some cancers (1–4). Some epidemiological studies have found that a high intake of green tea is associated with reduced risks of upper gastrointestinal tract cancer, mammary cancers, and primary liver cancer (5, 6). However, some epidemiological studies

have suggested that tea consumption might have adverse effects (7–11). Epidemiological studies conducted in Greece found no indication that intake of certain flavonoids reduced lung cancer risk, but an unexpected increased risk was observed (12). Higdon and Frei (13) reviewed many epidemiological studies on tea health and concluded that evidence regarding the effects of tea drinking on cancer and cardiovascular disease risk was conflicting. Further research on the underlying mechanisms of the bioactive ingredients of tea is required to improve our understanding of the association between tea consumption and health.

Competing Interest: The authors declare no competing interest.

Received: August 27, 2023. **Accepted:** January 5, 2024

© The Author(s) 2024. Published by Oxford University Press on behalf of National Academy of Sciences. This is an Open Access article distributed under the terms of the Creative Commons Attribution-NonCommercial-NoDerivs licence (<https://creativecommons.org/licenses/by-nc-nd/4.0/>), which permits non-commercial reproduction and distribution of the work, in any medium, provided the original work is not altered or transformed in any way, and that the work is properly cited. For commercial re-use, please contact journals.permissions@oup.com

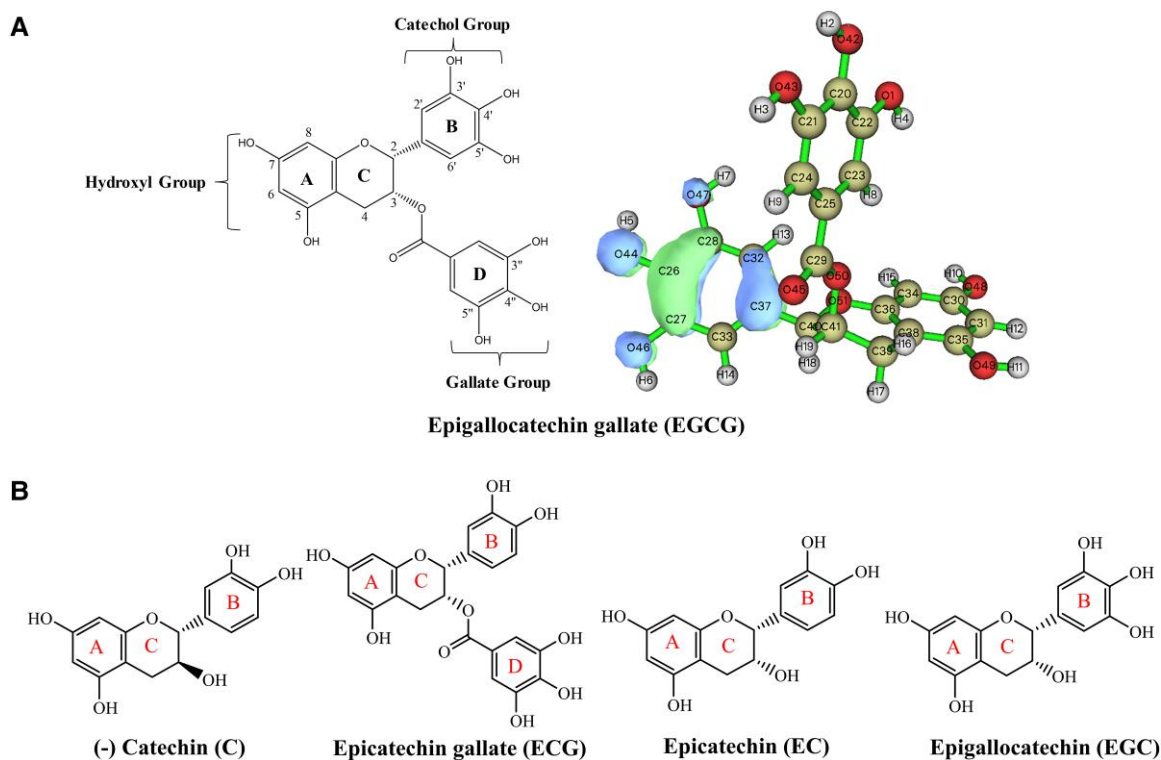


Fig. 1. Chemical structures of typical catechins in tea. A) EGCG with the highest occupied molecular orbital electron cloud density of the EGCG molecular frontier orbital. B) Catechin, epicatechin gallate, epicatechin, and epigallocatechin.

Epigallocatechin gallate (EGCG) is the dominant bioactive component in tea (3, 7). EGCG is widely used as an additive in food and beverages, health-care products, and clinical medicines (14), even though the Food and Drug Administration has stated that there is no credible evidence supporting the claim that tea drinking or EGCG can fight cancer (4). EGCG is a catechin (Fig. 1), which basically contains two functional groups that can produce free radicals. These are the catechol group (B ring) and the hydroxyl group (A ring). The formed free radicals can act as reducing agents and are responsible for the antioxidant ability of EGCG (13, 15–17). It has been reported that EGCG attenuates the progression of heart failure through a scavenging of free radicals and a reduction of cardiac chronic inflammation (18). EGCG can also affect transcription factors and enzymatic activity and thereby be beneficial for human health (17, 19). A daily intake of EGCG of 66.7 mg day^{-1} for an individual was derived in the European Prospective Investigation into Cancer and Nutrition–InterAct (EPIC interact) case–cohort study (20). However, an intake of EGCG and some other polyphenols was found to induce cleavage of the MLL gene, which could cause infant leukemia (21–23). Furthermore, an intake of a high dose of EGCG aggravated inflammation in mice with colitis and disturbed kidney function (19). Therefore, there are still many puzzles about the mechanisms and effects of EGCG as the most important active ingredient of tea.

Antioxidants, such as EGCG, work by quenching or removing harmful short-lived free radicals (24). Therefore, free radical chemistry is the core of understanding the health effects of EGCG. It is thought that EGCG can greatly decrease oxygen-free radicals in reperfusion injury in vivo (25, 26). However, the possible production of harmful free radicals from EGCG under actual environmental conditions has not been considered. Scenarios of afternoon tea exposure to outdoor sunlight are possibly prevalent in many people's daily lives. Whether harmful free radicals are

intensely produced beneath the calm surface of the cup of tea when people relax under outdoor sunlight has never been studied. Considering that free radicals and their reactions are playing very pivotal roles in many fields including food, environment, and human health, it is urgent to recognize the underlying free radical production and reactions in brewed tea.

Here, we used electron paramagnetic resonance (EPR) spectroscopy for in situ detection combined with quantum chemical computation to study free radical formation from EGCG of brewed tea under light irradiation (Fig. S1). The potential effects of the identified free radicals on DNA damage, cell cytotoxicity, and apoptosis were tentatively explored in vitro. Screening of the free radical–intermediated products was conducted by Fourier transform ion cyclotron resonance–mass spectrometry (FT-ICR MS) to further clarify the free radical formation and transformation pathways. It is expected to improve our further understanding of the free radical chemistry related to the widely used EGCG in food and beverages or brewed tea in human daily lives by conducting this study.

Results and discussion

Free radical formation from EGCG and other catechins contained in tea under simulated sunlight

EGCG and other catechins are widely contained in tea. Identification of free radicals formed from catechin could aid in further understanding the behavior and health effects of tea. Here, in-situ EPR spectroscopy detection was applied using 5,5-dimethyl-1-pyrroline-N-oxide (DMPO) as a spin-trapping agent to distinguish the potential free radical species formed from EGCG in brewed tea under light irradiation. This simulated

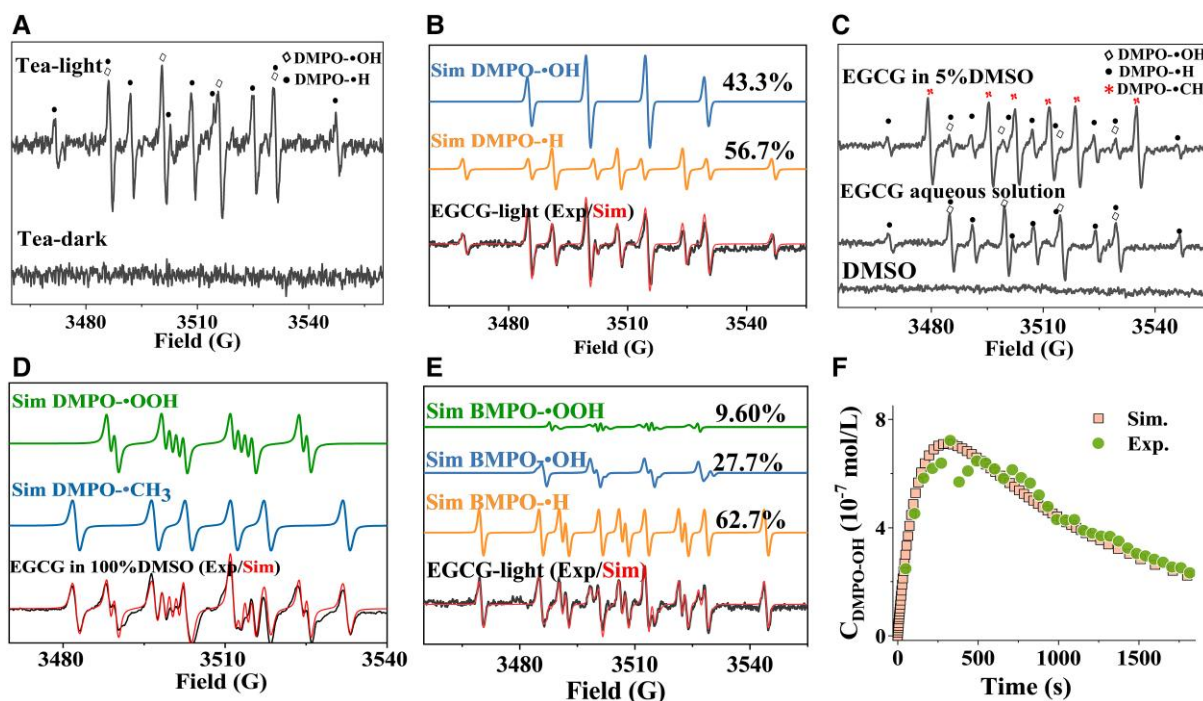


Fig. 2. Free radical identification in tea under sunlight. A) EPR spectra of DMPO-trapped radicals from brewed tea under full bandwidth light irradiation (100 mW cm^{-2}) and in the dark. B) The experimental (black line) and simulated EPR spectra (red line) of DMPO- \bullet OH and DMPO- \bullet H adducts. C) EPR spectra of DMPO-trapped radicals containing DMPO- \bullet OH, DMPO- \bullet H, and DMPO- \bullet CH₃ after the addition of 5% DMSO. D) The experimental and simulated EPR spectra of the DMPO- \bullet CH₃ and DMPO- \bullet OOH adducts with the addition of excess DMSO (100%). E) The experimental and simulated EPR spectra of the BMPO- \bullet OOH, BMPO- \bullet OH, and BMPO- \bullet H adducts. F) Kinetics of DMPO- \bullet OH yields from EGCG under light irradiation acquired by EPR spectroscopy and simulated by kinetic modeling using Kintecus software.

a real-world scenario of enjoying a leisurely afternoon tea outdoors in the sunshine. DMPO-hydroxyl radicals (\bullet OH) with a hyperfine splitting constant (hfsc) of $a_N = a_H = 14.8 \text{ G}$ (27) and DMPO-hydrogen radicals (\bullet H) with a hfsc of $a_N = 16.5 \text{ G}$ and $a_H = 22.5 \text{ G}$ (28, 29) were identified in both the brewed tea and the EGCG aqueous solution (Figs. 2A and S2A). A simulated spectrum of DMPO- \bullet OH and DMPO- \bullet H fit quite well with the experimental spectrum (Fig. 2B). The yields of \bullet H (43.3%) and \bullet OH (56.7%) were similar. DMPO- \bullet OH can be detected as an impurity when DMPO is added to a buffer because of the nucleophilic addition of water (30). Consequently, we conducted secondary radical spin-trapping experiments using 5% dimethyl sulfoxide (DMSO) as a typical \bullet OH scavenger to further confirm the existence of \bullet OH in the system (30–32). As shown in Fig. 2C, adding 5% DMSO to EGCG aqueous solution led to a decrease of DMPO- \bullet OH concentration and a corresponding increasing yield of DMPO- \bullet CH₃ adduct with a hfsc of $a_N = 16.3$, $a_H = 23.3 \text{ G}$ derived from DMSO and \bullet OH (Fig. 2C). These results were evidence of the presence of \bullet OH in the EGCG photochemical reaction system and in brewed tea. When an excess of DMSO was added to the system, the \bullet OH and \bullet H were all scavenged by the DMSO, and hyperfine splitting signals for DMPO- \bullet OOH ($a_N = 12.73$, $a_{H\beta} = 10.18 \text{ G}$, and $a_{H\gamma} = 1.30 \text{ G}$) were observed (Fig. 2D). This indicated that superoxide radicals ($\text{O}_2^{\bullet-}$) formed in the reaction system and could be stabilized by the DMSO. The stabilized $\text{O}_2^{\bullet-}$ was then trapped by DMPO (Fig. 2D) and easily transferred to DMPO- \bullet OOH in the DMSO solvent (33–35). The trapping agent 5-tert-butoxycarbonyl-5-methyl-1-pyrroline-N-oxide (BMPO) allows for the accumulation of EPR signals (27). When using BMPO as the spin-trapping agent, BMPO- \bullet OH (with a hfsc of $a_N = 14.07 \text{ G}$, $a_{H\beta} = 15.23 \text{ G}$, and $a_{H\gamma} = 1.27 \text{ G}$ for conformer I; $a_N = 14.12 \text{ G}$, $a_{H\beta} = 12.67 \text{ G}$, and $a_{H\gamma} = 0.67 \text{ G}$ for conformer II), BMPO

- \bullet H (with a hfsc of $a_N = 15.57 \text{ G}$, $a_{H\beta 1} = 20.81 \text{ G}$, and $a_{H\beta 2} = 22.29 \text{ G}$), and BMPO- \bullet OOH (with a hfsc of $a_N = 13.50 \text{ G}$ and $a_H = 12.10 \text{ G}$ for conformer I; $a_N = 13.30 \text{ G}$ and $a_H = 10.07 \text{ G}$ for conformer II) were observed (Figs. 2E and S2B). These results also indicated the production of \bullet OH, \bullet H, and $\text{O}_2^{\bullet-}$ in the light irradiation reaction system, occupying 27.7, 62.7, and 9.6% of the total active free radical production yield, respectively. Therefore, even though \bullet H is generated, significant concentrations of \bullet OH and few $\text{O}_2^{\bullet-}$ are also generated in both brewed tea and EGCG aqueous solutions under light irradiation. The spin concentrations of \bullet OH produced for each mole of EGCG were up to $2.4 \times 10^{-4} \text{ mol}$ (1.5×10^{20} spins), which was ~ 1.3 times that produced from hydrogen peroxide (H_2O_2 , $1.8 \times 10^{-4} \text{ mol}$) at the same molar amount under the same intensity of light irradiation. The first-order rate constant of \bullet OH from EGCG aqueous solution under light irradiation was estimated at $4.5 \times 10^{-4} \text{ s}^{-1}$ (Figs. 2F and S3 and Table S1), which was ~ 58 times that of photoinduced production of \bullet OH from H_2O_2 ($7.2 \times 10^{-6} \text{ M s}^{-1}$) (36). These results indicate significant production yield and the rate of \bullet OH from EGCG under light irradiation.

To date, a few studies have reported on the occurrences of \bullet OH (37) and H_2O_2 (38) under specific biological conditions in the presence of polyphenols (39). In earlier research, polyphenols, including EGCG, only produce \bullet OH if metal ions were present (40, 41). Interestingly, we found that significant formation of \bullet OH and \bullet H from EGCG and brewed tea occurred under sunlight irradiation without these specific biological conditions or metals. We subsequently investigated the 3T3-L1 cell viability (Fig. 3A), apoptosis (Figs. 3B, C and S4), and DNA damage (Fig. S5) in vitro after treating the cells with different concentrations of EGCG under light irradiation. A significant reduction ($P < 0.001$) in cell viability was found in the experimental group under light irradiation compared with

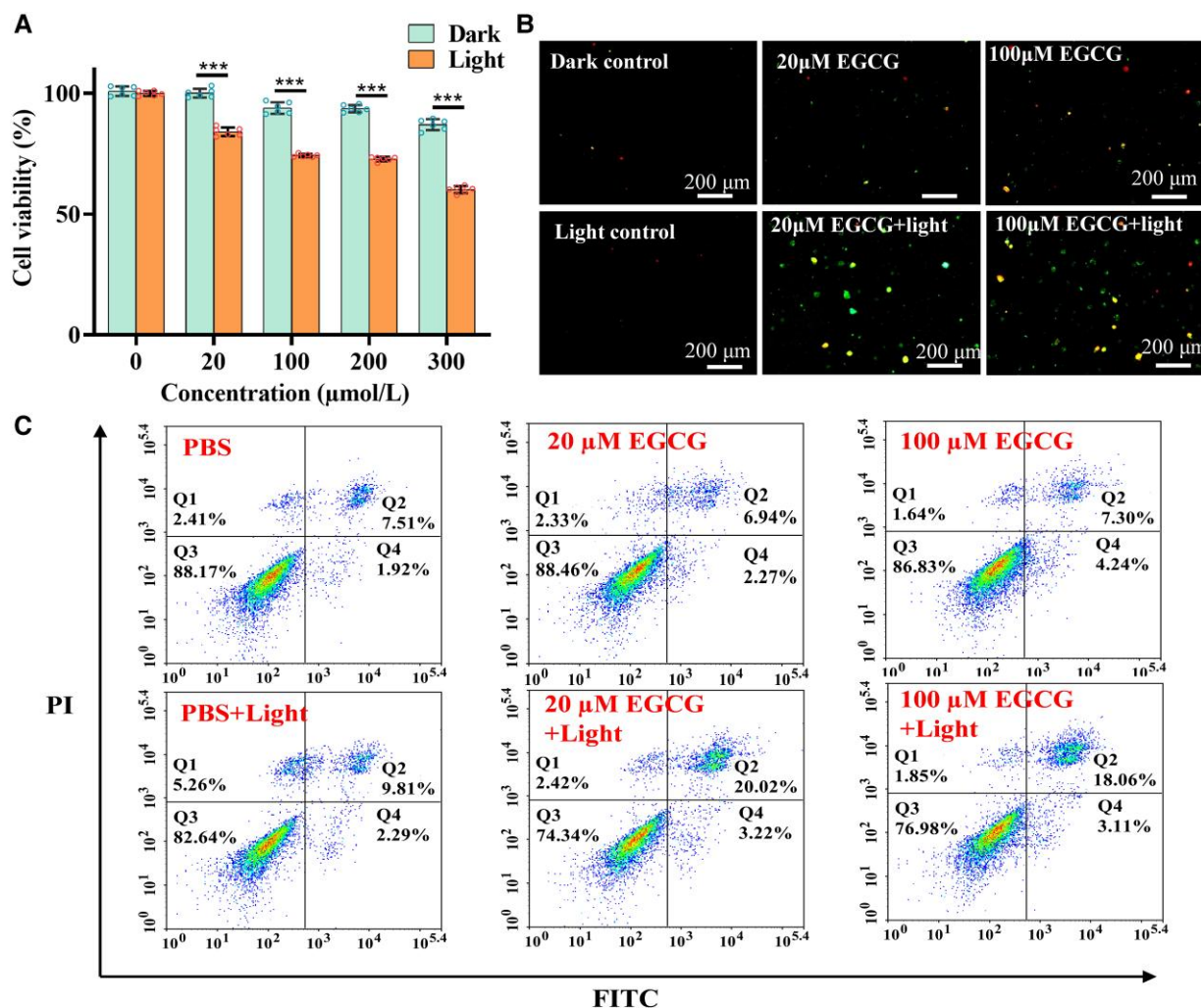


Fig. 3. Free radical cell cytotoxicity evaluation. A) The cell viability of 3T3-L1 cells was incubated with different concentrations of EGCG under light irradiation and in the dark. Data are presented as the mean \pm SD ($n = 6$). *** $P < 0.001$. B) Annexin V-FITC/PI costaining of 3T3-L1 cells treated with different concentrations of EGCG under light irradiation (70 mW cm^{-2}) and in the dark. C) Annexin V-FITC/PI showing cell apoptosis via flow cytometry.

the control group in the dark. The cells treated with EGCG under light irradiation showed distinct apoptosis, which was displayed as fluorescence both in the cytomembrane and cell nucleus (Figs. 3B, C and S4). The decrease in cell viability and observed apoptosis confirmed the instant effect of photoinduced free radicals, especially $\bullet\text{OH}$. Therefore, the benefits of drinking tea when it is exposed to sunlight merit further attention.

The conjugation effects of the A and B rings (Fig. 1A) in catechins are responsible for free radical formation. The alcohol hydroxyl group (C ring) is not an active group for free radical production because it cannot form a conjugated bond. The conjugation bond in the A ring is considered greater than that in the B ring because the A ring contains one more oxygen atom than the B ring (Fig. 1A and B). Therefore, the B ring is always more active for free radical formation than the other rings (13). The formed free radicals can act as reducing agents and are responsible for the antioxidant abilities of catechins (13, 15–17). We found that the capacities of different compounds to form $\bullet\text{OH}$ under light irradiation for 500 s were in the order of $\text{EC} > \text{ECG} > \text{C} > \text{EGCG} > \text{EGC}$ (Fig. 4A). The $\bullet\text{H}$ formation capacities were in the order of $\text{EC} > \text{C} > \text{EGC} > \text{ECG} > \text{EGCG}$ (Fig. 4B). These results indicate that there are different formation mechanisms and influencing factors for $\bullet\text{OH}$ and $\bullet\text{H}$ formations from catechins. For

the formation of $\bullet\text{OH}$, the conjugation effect was critical, and the three phenolic hydroxyl groups in EGCG and EGC could extend the π bond in the B ring, strengthen the carbon–oxygen bond, and decrease the yield of $\bullet\text{H}$ (Fig. 1). Therefore, the $\bullet\text{OH}$ yields from EGCG and EGC with three phenolic hydroxyl groups were lower than those from EC, ECG, and C with two phenolic hydroxyl groups (Fig. 4A). Additionally, steric effects determined the yield of $\bullet\text{H}$. This contributed to the lower yields of $\bullet\text{H}$ from ECG and EGCG compared with other catechins because they had more complicated configurations (Figs. 1 and 4B).

The direct scission of chemical bonds by UV irradiation is responsible for the photochemical formation of free radicals (36, 42). The wavelength and intensity of light irradiation are possibly important factors for free radical formation. We found that the continuous formation of $\bullet\text{H}$ and $\bullet\text{OH}$ occurred under constant light irradiation (Fig. 4C). The spin concentrations of $\bullet\text{H}$ were higher than those of $\bullet\text{OH}$, which could be attributed to the conjugated π bonds in the A and B rings (Fig. 1) strengthening the carbon–oxygen bond and making dehydrogenation easier. Additionally, formations of those free radicals, dependent on specific light irradiation as EPR silent, are observed during visible light irradiation (Fig. 4D). The concentrations of the free radicals were also dependent on the irradiation intensity (Fig. 4E and F). The wavelength

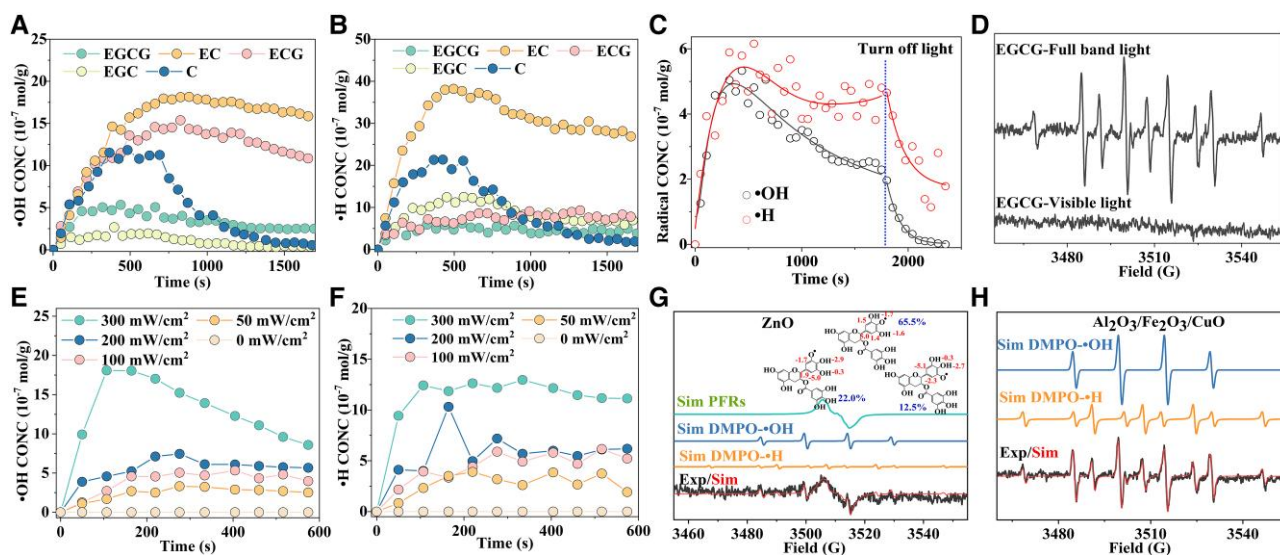


Fig. 4. Influence factors for •OH and •H production from EGCG as an active ingredient in tea. A and B) Dynamic changes in the yields of photoinduced •OH and •H from typical catechins in tea as a function of the irradiation time. C) Dynamic changes in the yields of photoinduced radicals produced from EGCG as a function of irradiation time, along with the temporal decay of radicals subsequent to light cessation. D) DMPO adducts formed when an EGCG aqueous solution was irradiated with full bandwidth light and visible light. E and F) Concentrations of •OH and •H produced from EGCG under light irradiation with different intensities. G) The experimental and simulated EPR spectra for DMPO-•H, DMPO-•OH, and persistent-free radicals formed when ZnO was added to the photochemical reaction system. H) The experimental and simulated EPR spectra for DMPO-•H and DMPO-•OH when Al₂O₃, Fe₂O₃, and CuO were added to the photochemical reaction system.

(300–1,100 nm) and intensity (100 mW cm⁻²) of the xenon lamp used for the laboratory photochemical experiments fall within the range of sunlight (300–1,800 nm and ≤100 mW cm⁻²; Fig. S6). Therefore, the wavelength and illumination intensity of sunlight could be responsible for •H and •OH formations in brewed tea, which could have practical environmental implications.

The metal oxide ZnO is frequently present in tea samples, contributing to 64% (48 mg kg⁻¹) of the total metal oxides, and is found in higher concentrations than Al₂O₃, Fe₂O₃, and CuO (Table S2). Therefore, we evaluated the influence of ZnO on free radical formation. In ZnO acetate buffer, specific persistent free radicals (Fig. 4G) did not form in Fe₂O₃, Al₂O₃, and CuO systems (Fig. 4H). This reflects the distinguished stabilization effect of ZnO on the organic free radicals simultaneously generated with •H and •OH from catechins. This result agrees with the previous study that the ZnO surface rich in delocalized π electrons above the benzene ring made the organic free radicals stable (43). The ZnO-stabilized organic free radicals were deconvoluted as semiquinone radicals formed by •H abstraction from the B ring (Fig. 4G). These stable semiquinone radicals may form covalent bonds with proteins and pose toxic effects to organisms (44, 45).

In this study, besides the formation of free radical •H, we discover the significant formation of •OH from EGCG and in brewed tea under light irradiation. Those easily formed free radicals may break the free radical equilibrium in human and are responsible for the ambiguous effects of tea consumption when exposed to outdoor sunlight. In addition to these reactive free radicals, the simultaneously formed organic free radicals can be stabilized by ZnO and pose potential risks to human health.

Formation mechanisms of free radicals from EGCG as an active ingredient in tea

We used FT-ICR MS for screening the free radical-intermediated products to clarify the formation mechanisms of free radicals produced from EGCG under light irradiation. Both photooxidation

products and photoreduction products produced from EGCG were detected. These compounds were characterized by plotting the carbon oxidation state (Osc = 2O/C–H/C) against the carbon number (Fig. 5A). Unsurprisingly, during the photoreaction of EGCG in vitro, the Osc values of most of the molecular products were <0.182, which is the Osc value of EGCG. Some of the Osc values were even below zero, which indicated that photoreduction reactions were dominant in the system.

The B ring of EGCG was more prone to produce •H because of its weaker oxygen–hydrogen bond compared with the A ring (pathway A in Fig. 5B) (46), which was attributed to the weaker conjugation effect of the B ring compared with the A ring (13). Additionally, we considered that steric hindrance had a significant influence on the •H yield from catechins. Currently, there is no study pointing out the simultaneous formation of •OH, which is the most damaging free radicals in biosystems (24), not to mention their formation mechanisms. The products with the highest responses were the photooxidation products (e.g. C₂₂H₁₈O₁₂, *m/z* 473.0725) and the photoreduction products (e.g. C₂₂H₁₈O₁₀, *m/z* 441.0827), which were produced from EGCG (C₂₂H₁₈O₁₁) in reactions involving •OH (Fig. 5B). The lowest •OH yields were obtained with EGCG and EGC, which indicated that •OH formation was dependent on the conjugation effect of the B ring. Therefore, the B ring is the dominant donor for •OH in the reaction system as for •H. The one O reduction product at *m/z* 441.0827 (C₂₂H₁₈O₁₀) may be responsible for •OH production from EGCG, followed by •H coupling. Therefore, during light irradiation, we speculated that homolytic decomposition of the C–O bond in the B ring of EGCG could occur. This would lead to the formation of •OH and carbon-centered organic radicals, which could subsequently couple with •H (pathway B in Fig. 5B). The carbon-centered organic radicals could not be detected by EPR spectroscopy in the aqueous reaction because of the •H coupling reaction; however, they could be stabilized by metal oxides (e.g. ZnO). EPR signals for these organic radicals on ZnO were detected (Fig. 4G). Additionally, O₂⁻, which was trapped by both DMPO and

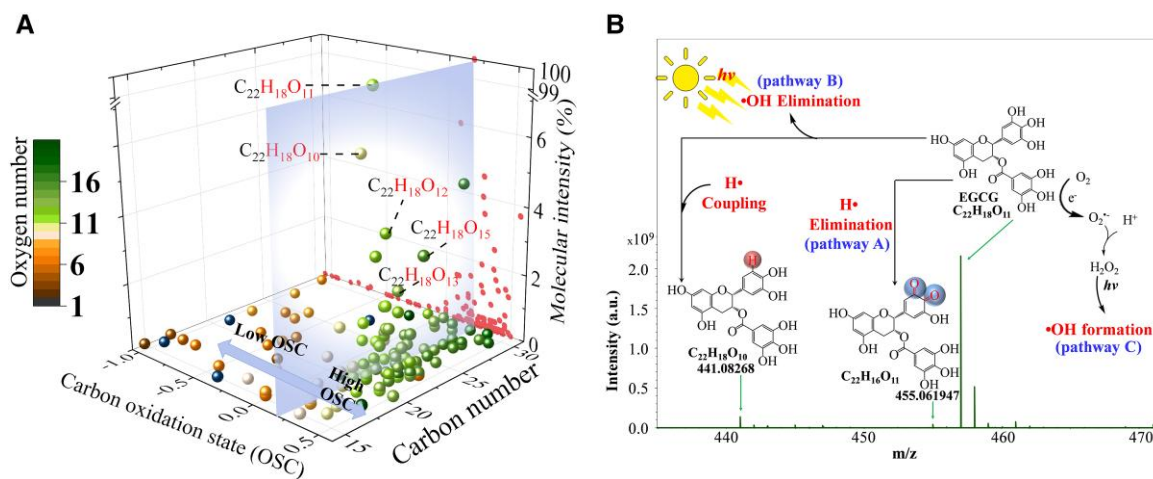


Fig. 5. Mechanisms of $\bullet\text{OH}$ and $\bullet\text{H}$ formation from EGCG as an active ingredient in tea. A) Chemical characterization of the molecular products formed during photooxidation of EGCG in a plot of the carbon oxidation state (OSC) vs. the carbon number. B) Observed formation of EGCG-related products using FT-ICR MS, and the proposed mechanisms for $\bullet\text{OH}$ and $\bullet\text{H}$ formation from EGCG under light irradiation.

BMPO in this study (Figs. 2D and S2), could also easily form through electron transfer from these organic free radicals to O_2 (42, 47). Then, $\text{O}_2^{\bullet-}$ could transfer to H_2O_2 , which could decompose homolytically to form $\bullet\text{OH}$ (pathway C in Fig. 5B). To further explore the influence of O_2 on $\bullet\text{OH}$ formation, deoxygenation was conducted in the reaction system. As a result, the yield of $\bullet\text{OH}$ decreased to 83.3% of the original yield (Fig. S7), indicating the contribution of pathway C to the formation of $\bullet\text{OH}$.

In summary, by combining in situ EPR spectroscopy of the free radicals and FT-ICR MS of the molecular products from EGCG as an active ingredient in tea under light irradiation, we have obtained evidence of the production of $\bullet\text{OH}$ in brewed tea under light irradiation. Additionally, we have proposed a formation mechanism involving breaking of the O–H bond in phenolic OH groups on the B ring to form $\bullet\text{H}$ radicals and breaking of the C–O bonds on the B ring and D ring to form $\bullet\text{OH}$ radicals. This is followed by singlet electron transfer from EGCG to O_2 to form $\text{O}_2^{\bullet-}$ and H_2O_2 . The H_2O_2 then decomposes to generate $\bullet\text{OH}$ under light irradiation.

Free radicals and their reactions are playing very pivotal roles in many fields including food, environment, and human health. For example, free radical theory is considered the underlying mechanism of human aging and disease (48–50). Excess free radicals, specifically $\bullet\text{OH}$, could cause lipid peroxidation and lead to lipid membrane damage. If this reaction is not controlled in a timely manner, $\bullet\text{OH}$ might continuously damage cellular membranes in a chain reaction involving the extraction of electrons and production of lipid-free radicals (51). Furthermore, $\bullet\text{OH}$ could cause oxidative stress and DNA damage and therefore decrease cell viability. In this study, EGCG as the active ingredient in tea effectively produced $\bullet\text{OH}$ under light irradiation. This is important because $\bullet\text{OH}$ is considered the most damaging free radical in biological systems. The discovery of $\bullet\text{OH}$ production in brewed tea under sunlight in this study suggests that much more extensive research on their potential practical application and health implications should be conducted.

The human body is a highly complex and sophisticated system, and the impact of the discovery of $\bullet\text{OH}$ in brewed tea on human health is still not fully clarified. The oxidative stress caused by $\bullet\text{OH}$ in brewed tea is unclear, as it could either have damaging or beneficial effects. Variables such as an individual's fitness level, tea-drinking scenario, tea type, and active ingredient content, among others, can all influence their effects on health. However, it is

generally believed that drinking tea polyphenols is beneficial to the health of the general population. Nevertheless, the discovery of $\bullet\text{OH}$ in brewed tea is undoubtedly interesting, as it serves as a significant clue that drinking tea under sunlight irradiation should be taken into consideration. Additionally, the potential applications and implications of the relatively mild $\bullet\text{OH}$ produced from brewed tea under light irritations in various fields are worth exploiting.

Materials and methods

Characterization of the tea samples

The tea samples used in this study consisted of green tea varieties, procured from a local supermarket in Beijing, China. The dry weight of the tea samples was found to contain ~15% EGCG (LC purity $\geq 92.9\%$, Dr Ehrenstorfer GmbH). For the analysis of metal elements in tea, tea samples were characterized using inductively coupled plasma mass spectrometry (ICP MS-2030, SHIMADZU, Germany). Each green tea (1 g) sample was digested using 8 mL of aqua regia (69% HNO_3 :36% HCl) in a microwave digestion system for sample preparation for metal detection by ICP-MS. The digestion program was as follows: 120 °C for 5 min under 500 W microwave power, 160 °C for 10 min under 500 W microwave power, and 180 °C for 20 min under 700 W microwave power. The sample was then cooled to 50 °C. After acid treatment, the digestion tank was removed, and the solvent was exchanged with deionized water. The sample was diluted to 10 mL and filtered through a 0.45- μm polytetrafluoroethylene filter. Finally, the sample was injected into the inductively coupled plasma mass spectrometer for the determination of the heavy metal contents. The contents of zinc, aluminum, and copper in the tea samples were relatively high (Table S2). The effects of ZnO , Al_2O_3 , Fe_2O_3 , and CuO on free radical formation were evaluated.

Identification, quantification, and formation kinetics of free radicals produced from EGCG and brewed tea under light irradiation

EGCG is the dominant ingredient in tea. Free radical species produced from an EGCG aqueous solution under sunlight irradiation were detected. We prepared brewed tea at 90 °C for 5 min, followed by implementing a nondestructive, in situ irradiation technique using EPR spectroscopy (EMX plus, Bruker Instruments,

USA) equipped with a light source to simulate free radical formation in brewed tea under light irradiation (Fig. S1). Both DMPO (GC purity $\geq 99\%$, Dojindo Molecular Technology, Japan) and BMPO (GC purity $\geq 99\%$, Dojindo Molecular Technology) were used for reactive free radical trapping during the photochemical reaction. EPR spectroscopy was used to measure the formation of active free radicals, including $\bullet\text{OH}$ and $\bullet\text{H}$. No evidence of an EPR signal was observed in pure water, DMPO, or BMPO under the same conditions (Figs. 2C and S2A and B), suggesting that the observed radicals were derived from brewed tea and EGCG under light irradiation. The hfsc and line characteristics of DMPO and BMPO spin-trapping adducts were used to identify the free radicals. EPR secondary radical spin trapping with DMSO as a typical $\bullet\text{OH}$ scavenger was used for further confirmation of the existence of $\bullet\text{OH}$ (30–32, 52).

The hfscs of the free radicals were evaluated using Bruker's Xenon program. The hfscs can reflect the magnetic interaction between the nucleus and the electron (27). Density functional theory was used for the calculation of hfsc. The structures of the ground states of the EGCG-related radicals were optimized using the unrestricted hybrid functional B3LYP and the 6-31G* basis sets. The hfscs were calculated using the B3LYP functional and the EPR-II basis sets with B3LYP/6-31G* geometry. The calculated hfscs of the EGCG-related radicals were elucidated using the Xenon program to fit the original EPR spectrum.

Radical quantification was conducted using Bruker's Xenon program according to the quantitative theory of spin calculation. Absolute values of the spins in the samples were calculated using the following equation:

$$DI = \frac{c}{f(B_1, B_m)} \times [G_R \times G_t \times n] \times [\sqrt{P} \times B_m \times Q \times n_B \times S \times (S + 1)] \times n_S$$

where DI is the result of double integration of the EPR signal, G_R is the receiver gain, G_t is the conversion time (s), P is the microwave power (W), B_m is the modulation amplitude (G), n_B is the Boltzmann factor for temperature dependence, S is the total electron spin, n is the number of scans, and Q is the quality factor of the resonator. The factors described above were all known during the detection by EPR spectroscopy. In addition, n_S is the number of spins, c is the point sample sensitivity calibration factor, and $f(B_1, B_m)$ is the resonator volume sensitivity distribution. The value of $c/f(B_1, B_m)$ was obtained through factory calibration. The above radical quantification method was developed in consultation with the design engineer of Bruker's Xenon program and is described in our previous study (53). The precision of Bruker's Xenon program for radical quantification was tested by comparison of the experimental data with the calculated data.

Metal oxides are common in tea and may influence the formation of free radicals from EGCG under light irradiation. Here, EGCG aqueous solution containing the metal oxides, which are of relatively higher contents in practical tea samples, such as ZnO, Al_2O_3 , CuO, and Fe_2O_3 (99.9% purity, Sigma-Aldrich, Co., St Louis, MO, USA), were evaluated for their free radical generation capacity. The pH is also important for free radical formation. The concentrations and species of free radicals formed in EGCG aqueous solutions with different pH values varied (Fig. S8A). We found that $\bullet\text{OH}$ could form in EGCG aqueous solutions over a wide pH range (pH 2–11). In a strongly alkaline environment (pH 12), organic free radicals and $\bullet\text{H}$ formed. Simulation of the hyperfine signals of organic free radicals demonstrated that semiquinone radicals were generated (Fig. S8B) after $\bullet\text{H}$ abstraction from the B ring of EGCG. Considering that brewed tea is neutral or weakly acidic, the experimental pH was

adjusted to 7.4 using phosphate-buffered saline (PBS). All reactions were carried out using the following reagents: 2 μL of 3 M DMPO, 30 μL of 1 \times PBS (0.01 M, pH 7.4), and 20 μL of 2 mg mL^{-1} EGCG/metal oxide (ZnO, Al_2O_3 , CuO, Fe_2O_3 , or no metal oxide).

Free radicals produced from EGCG under light irradiation were detected in situ using X-band EPR with a xenon lamp of 100 mW cm^{-2} light irradiation (CHF-XM500, Perfectlight, China) to simulate sunlight. The xenon lamp spectrum was like that of real sunlight (Fig. S6). The EPR parameters were as follows: microwave frequency, 9.78 GHz; modulation frequency, 100 kHz; modulation amplitude, 1.0 G; receiver gain, 10 dB; center field, 3,505 G; sweep width, 100 G; time constant, 81.92 ms; sweep time, 50 s; and microwave power, 20 mW.

We used a kinetic model to obtain the rate constants of reactive species produced from EGCG under light irradiation. The concentrations of the reactive species were simulated by kinetic modeling using Kintecus software. The kinetic model included the formation reactions, coupled reactions, and additional reactions related to photoinduced free radical production from EGCG. Details for the reactions are shown in Table S1.

Screening of photochemical reaction products from EGCG as an active ingredient of tea by FT-ICR MS

Photochemical reaction products of the EGCG as an active ingredient of tea were screened using FT-ICR MS (Solarix-15T, Bruker, Germany) in negative ionization mode (Fig. S1). Before analysis, 3 mL of an aqueous EGCG solution (2 g L^{-1}) or brewed tea (20 g L^{-1}) was irradiated under a xenon lamp for 1 h. For FT-ICR MS, an aliquot (3 μL) of the irradiated solution was diluted in 600 μL methanol/water (1:1, v/v). The instrument was equipped with a 15.0-T magnetic field. The screening mass range was m/z 0–1,500. The atomizer temperature was set at 300 $^\circ\text{C}$, the drying temperature was 220 $^\circ\text{C}$, and the drying gas flow rate was 4.0 L min^{-1} . The ion accumulation time was 0.01 s, and the capillary inlet voltage was -3.8 kV. Sodium formate (10 mmol L^{-1}) was used as the calibration solution. The mass error after calibration was <1 ppm. DataAnalysis 5.0 was used for molecular assignment. The signal-to-noise ratio was set at 6. The relative peak area threshold was 0.1%, the relative peak intensity threshold was 0.01%, and the relative intensity threshold was 0.01%. The absolute intensity was 10,000. The elemental composition was set as $\text{C}_x\text{H}_y\text{O}_z$. The error of the molecular assignment was set to <1 ppm. Molecular formulae that overlapped between the blanks and samples were excluded.

In vitro experiments to evaluate DNA damage, cell cytotoxicity, and apoptosis induced by free radicals produced from EGCG as an active ingredient of tea under light irradiation

3T3-L1 cells were used as the model cells for in vitro experiments to assess DNA damage, cell cytotoxicity, and apoptosis induced by free radicals produced from EGCG under light irradiation. The 3T3-L1 cells were grown in Dulbecco's modified Eagle's medium at 37 $^\circ\text{C}$ under a 5% CO_2 atmosphere. The cells were cultured in a medium containing 10% fetal bovine serum and 1% penicillin streptomycin.

In vitro cytotoxicity assays of the free radicals produced from EGCG were conducted by assessing the cell viability of 3T3-L1 cells. 3T3-L1 cells were seeded in 96-well plates at a density of $1\text{--}1.5 \times 10^4$ cells per well. The cells were incubated at 37 $^\circ\text{C}$ overnight. After incubation with different concentrations of EGCG for 0.5 h, the cells were then irradiated with full bandwidth light (70 mW cm^{-2} , 15 min). The treated cells were then cultured for

an additional 24 h. Cells in the control group were treated in the same manner, except for exposure to light. Finally, the cell viability was determined using a cell counting kit-8 (CCK-8, Dojindo Molecular Technology) following a standard protocol. The absorbance for the Bio-Rad microplate reader was set at 490 nm.

In vitro cell death analysis was conducted using Annexin V-FITC/propidium iodide (PI) immunofluorescence. An Annexin V-FITC/PI Apoptosis Detection Kit (Elabscience, China) was used for the detection of photoinduced cell death caused by free radicals produced from EGCG under light irradiation. 3T3-L1 cells were seeded onto 20-mm confocal dishes for 24 h. The cells were then incubated with PBS, 20 μM EGCG, and 100 μM EGCG for 30 min, respectively. After this, the cells were irradiated with full bandwidth light (70 mW cm^{-2} , 15 min). The irradiated cells were stained with the Annexin V-FITC/PI Apoptosis Detection Kit for 15 min and visualized by fluorescence microscopy (DMI8, Leica, Germany) with an excitation wavelength of 488 nm. The emission wavelength was measured from 505 to 545 nm (green channel) and from 600 to 700 nm (red channel). In addition, a flow cytometer (BD FACS LSR II, BD Biosciences, USA) was used to quantitatively show cell necrosis and apoptosis degree. The cells in the control group were treated in the same manner, except for exposure to light.

In vitro DNA damage was assessed using phosphorylation of H2AX at Ser 139 (γ -H2AX) immunofluorescence analysis. We used γ -H2AX to probe the formation of DNA double-strand breaks with EGCG after light irradiation. 3T3-L1 cells were seeded on 20-mm confocal dishes at a density of 5×10^4 cells for 24 h. The cells were incubated with PBS, 20 μM EGCG, or 100 μM EGCG for 30 min. Next, the cells were irradiated with full bandwidth light (70 mW cm^{-2} , 15 min). The irradiated cells were cultured for an additional 7 h, washed with PBS, and fixed with paraformaldehyde for 10 min. After rinsing with PBS, the fixed cells were permeabilized with Triton-X 100 for 15 min at room temperature. Subsequently, the cells were incubated with γ -H2AX Ab (Beyotime Biotechnology, China) overnight at 4 $^{\circ}\text{C}$. After washing, the cells were stained with the secondary antibody antirabbit Alexa-488 (Beyotime Biotechnology) for 1 h at room temperature. The cell nuclei were stained with DAPI for 5 min at room temperature, followed by the addition of an antifade mounting medium. Finally, the cells were imaged under a confocal microscope (TCS SP5, Leica) with the following excitation and emission wavelengths: 350 and 460 nm for DAPI and 488 and 525 nm for Alexa-488. The cells in the control group were treated in the same manner, except for exposure to light.

Supplementary Material

Supplementary material is available at PNAS Nexus online.

Funding

This work was funded by the National Natural Science Foundation of China (grant nos. 92143201, 21936007, and 22076201), Second Tibetan Plateau Scientific Expedition and Research Program (STEP; grant no. 2019 QZKK0605), and the CAS Interdisciplinary Innovation Team (grant no. JCTD-2019-03).

Author Contributions

G.L., M.Z., and G.J. conceptualized the project. L.Q., G.L., and L.Y. designed the methodology of the research. L.Q., L.Y., Y.Y., and S.L. performed the experiments. L.Q. and L.Y. performed the data analysis and visualized the experimental results. G.L. and

M.Z. performed the funding acquisition. G.L., M.Z., and G.J. administrated and supervised the work. L.Q., G.L., and L.Y. wrote the first draft. G.L., L.Y., C.S., M.S., F.F., and H.Z. reviewed and helped editing the manuscript.

Data Availability

The hyperfine splitting values of DMPO and BMPO adducts used in this study are available from the National Institute of Environmental Health Sciences (<http://tools.niehs.nih.gov/stdb/index.cfm>). The kinetic model included the chemical reactions related to photoinduced free radical production from EGCG and is obtained from Kintecus (<http://www.kintecus.com/>). The rate constant of the chemical reactions shown in Table S2 is available from NDRL/NIST Solution Kinetics Database on the Web (<https://kinetics.nist.gov/solution/>). All study data are included in the article and/or supplementary material.

References

- Sharma VK, Bhattacharya A, Kumar A, Sharma HK. 2007. Health benefits of tea consumption. *Trop J Pharm Res.* 6:785–792.
- Pinto MD. 2013. Tea: a new perspective on health benefits. *Food Res Int.* 53:558–567.
- Eisenstein M. 2019. Tea for tumours. *Nature.* 566:S6–S7.
- Anonymous. 2008. A teacupful of medicine? *Nat Struct Mol Biol.* 15:537–537.
- Yuan JM, Sun C, Butler LM. 2011. Tea and cancer prevention: epidemiological studies. *Pharmacol Res.* 64:123–135.
- Fon Sing M, Yang WS, Gao S, Gao J, Xiang YB. 2011. Epidemiological studies of the association between tea drinking and primary liver cancer: a meta-analysis. *Eur J Cancer Prev.* 20:157–165.
- Gilbert N. 2019. Drink tea and be merry. *Nature.* 566:S8–S9.
- De Bacquer D, Clays E, Delanghe J, De Backer G. 2006. Epidemiological evidence for an association between habitual tea consumption and markers of chronic inflammation. *Atherosclerosis.* 189:428–435.
- Hou IC, Amarnani S, Chong MT, Bishayee A. 2013. Green tea and the risk of gastric cancer: epidemiological evidence. *World J Gastroenterol.* 19:3713–3722.
- Arts IC. 2008. A review of the epidemiological evidence on tea, flavonoids, and lung cancer. *J Nutr.* 138:1561S–1566S.
- Tang N, Wu Y, Zhou B, Wang B, Yu R. 2009. Green tea, black tea consumption and risk of lung cancer: a meta-analysis. *Lung Cancer.* 65:274–283.
- Lagiou P, et al. 2004. Flavonoid intake in relation to lung cancer risk: a case-control study among women in Greece. *Nutr Cancer.* 49:139–143.
- Higdon JV, Frei B. 2003. Tea catechins and polyphenols: health effects, metabolism, and antioxidant functions. *Crit Rev Food Sci Nutr.* 43:89–143.
- Lecumberri E, Dupertuis YM, Miralbell R, Pichard C. 2013. Green tea polyphenol epigallocatechin-3-gallate (EGCG) as adjuvant in cancer therapy. *Clin Nutr.* 32:894–903.
- Guo Q, et al. 1999. ESR study on the structure-antioxidant activity relationship of tea catechins and their epimers. *Biochim Biophys Acta.* 1427:13–23.
- Jovanovic SV, Steenken S, Tosic M, Marjanovic B, Simic MG. 1994. Flavonoids as antioxidants. *J Am Chem Soc.* 116:4846–4851.
- Avendaño C, Menéndez JC. 2008. Cancer chemoprevention. In: *Medicinal chemistry of anticancer drugs.* Elsevier Science. p. 417–429.
- Oyama J, Komoda H, Node K, Makino N. 2012. Epigallocatechin gallate attenuates the progression of heart failure induced by

- heart/muscle-specific deletion of Mn-SOD in mice through scavenging free radicals and improving the cardiac chronic inflammation. *Circulation*. 126:A12801–A12801.
- 19 Asakura H, Kitahora T. 2018. Antioxidants and polyphenols in inflammatory bowel disease: ulcerative colitis and Crohn disease. In: Watson RR, Preedy VR, Zibadi S, editors. *Polyphenols: prevention and treatment of human disease*. New York: Academic Press. p. 279–292.
 - 20 Zamora-Ros R, et al. 2014. Dietary intakes of individual flavanols and flavonols are inversely associated with incident type 2 diabetes in European populations. *J Nutr*. 144:335–343.
 - 21 Strick R, Strissel PL, Borgers S, Smith SL, Rowley JD. 2000. Dietary bioflavonoids induce cleavage in the MLL gene and may contribute to infant leukemia. *Proc Natl Acad Sci U S A*. 97:4790–4795.
 - 22 Bais HP, Vepachedu R, Gilroy S, Callaway RM, Vivanco JM. 2003. Allelopathy and exotic plant invasion: from molecules and genes to species interactions. *Science*. 301:1377–1380.
 - 23 Mozaffarian D. 2021. Nutrition's dark matter of polyphenols and health. *Nature Food*. 2:139–140.
 - 24 Jovanovic SV, Hara Y, Steenken S, Simic MG. 1995. Antioxidant potential of gallic acid—a pulse-radiolysis and laser photolysis study. *J Am Chem Soc*. 117:9881–9888.
 - 25 Valcic S, Burr JA, Timmermann BN, Liebler DC. 2000. Antioxidant chemistry of green tea catechins. New oxidation products of (-)-epigallocatechin gallate and (-)-epigallocatechin from their reactions with peroxy radicals. *Chem Res Toxicol*. 13:801–810.
 - 26 Buttemeyer R, et al. 2003. Epigallocatechin gallate can significantly decrease free oxygen radicals in the reperfusion injury in vivo. *Transplant Proc*. 35:3116–3120.
 - 27 Feng GD, et al. 2016. Accelerated crystallization of zeolites via hydroxyl free radicals. *Science*. 351:1188–1191.
 - 28 Makino K, Mossoba MM, Riesz P. 1982. Chemical effects of ultrasound on aqueous-solutions—evidence for .OH and .H by spin trapping. *J Am Chem Soc*. 104:3537–3539.
 - 29 Buettner GR. 1987. Spin trapping: ESR parameters of spin adducts. *Free Radic Biol Med*. 3:259–303.
 - 30 Mason RP, Hanna PM, Burkitt MJ, Kadiiska MB. 1994. Detection of oxygen-derived radicals in biological-systems using electron-spin-resonance. *Environ Health Perspect*. 102:33–36.
 - 31 Zhu BZ, Kalyanaraman B, Jiang GB. 2007. Molecular mechanism for metal-independent production of hydroxyl radicals by hydrogen peroxide and halogenated quinones. *Proc Natl Acad Sci U S A*. 104:17575–17578.
 - 32 Zhu BZ, Zhao HT, Kalyanaraman B, Frei B. 2002. Metal-independent production of hydroxyl radicals by halogenated quinones and hydrogen peroxide: an ESR spin trapping study. *Free Radic Biol Med*. 32:465–473.
 - 33 Wei J, et al. 2021. Superoxide formation from aqueous reactions of biogenic secondary organic aerosols. *Environ Sci Technol*. 55:260–270.
 - 34 Huang YN, et al. 2019. Significant contribution of metastable particulate organic matter to natural formation of silver nanoparticles in soils. *Nat Commun*. 10:3775.
 - 35 Courtney CM, et al. 2017. Potentiating antibiotics in drug-resistant clinical isolates via stimuli-activated superoxide generation. *Sci Adv*. 3:e1701776.
 - 36 Stefan MI, Hoy AR, Bolton JR. 1996. Kinetics and mechanism of the degradation and mineralization of acetone in dilute aqueous solution sensitized by the UV photolysis of hydrogen peroxide. *Environ Sci Technol*. 30:2382–2390.
 - 37 Li ASH, Bandy B, Tsang SS, Davidson AJ. 2000. DNA-breaking versus DNA-protecting activity of four phenolic compounds in vitro. *Free Radic Res*. 33:551–566.
 - 38 Long LH, Clement MV, Halliwell B. 2000. Artifacts in cell culture: rapid generation of hydrogen peroxide on addition of (-)-epigallocatechin, (-)-epigallocatechin gallate, (+)-catechin, and quercetin to commonly used cell culture media. *Biochem Biophys Res Commun*. 273:50–53.
 - 39 Jeong JY, et al. 2015. Epigallocatechin-3-gallate-induced free-radical production upon adipogenic differentiation in bovine bone-marrow mesenchymal stem cells. *Cell Tissue Res*. 362:87–96.
 - 40 Hagerman AE, Dean RT, Davies MJ. 2003. Radical chemistry of epigallocatechin gallate and its relevance to protein damage. *Arch Biochem Biophys*. 414:115–120.
 - 41 Gligorovski S, Strekowski R, Barbati S, Vione D. 2015. Environmental implications of hydroxyl radicals ($\cdot\text{OH}$). *Chem Rev*. 115:13051–13092.
 - 42 Lee JK, et al. 2019. Spontaneous generation of hydrogen peroxide from aqueous microdroplets. *Proc Natl Acad Sci U S A*. 116:19294–19298.
 - 43 Liu S, Liu G, Yang L, Li D, Zheng M. 2022. Critical influences of metal compounds on the formation and stabilization of environmentally persistent free radicals. *Chem Eng J*. 427:131666.
 - 44 Zhang X, et al. 2020. Short-term exposure to ZnO/MCB persistent free radical particles causes mouse lung lesions via inflammatory reactions and apoptosis pathways. *Environ Pollut*. 261:114039.
 - 45 Pryor WA, Hales BJ, Premovic PI, Church DF. 1983. The radicals in cigarette tar—their nature and suggested physiological implications. *Science*. 220:425–427.
 - 46 Yassin GH, Koek JH, Kuhnert N. 2015. Model system-based mechanistic studies of black tea thearubigin formation. *Food Chem*. 180:272–279.
 - 47 Yu WC, et al. 2022. Unexpected persistent production of reactive oxygen species during the degradation of black phosphorus in the darkness. *Angew Chem Int Ed*. 61:e202213595.
 - 48 Harman D. 1956. Aging: a theory based on free radical and radiation chemistry. *J Gerontol*. 11:298–300.
 - 49 Zannoni N, et al. 2022. The human oxidation field. *Science*. 377:1071–1077.
 - 50 Thomas T, Thomas G, McLendon C, Sutton T, Mullan M. 1996. β -Amyloid-mediated vasoactivity and vascular endothelial damage. *Nature*. 380:168–171.
 - 51 Mylonas C, Kouretas D. 1999. Lipid peroxidation and tissue damage. *In Vivo*. 13:295–309.
 - 52 Gao HY, et al. 2020. First direct and unequivocal electron spin resonance spin-trapping evidence for pH-dependent production of hydroxyl radicals from sulfate radicals. *Environ Sci Technol*. 54:14046–14056.
 - 53 Yang L, et al. 2017. Molecular mechanism of dioxin formation from chlorophenol based on electron paramagnetic resonance spectroscopy. *Environ Sci Technol*. 51:4999–5007.